Charge sensing amplification via weak values measurement

Oded Zilberberg,[1] Alessandro Romito,[2,3] and Yuval Gefen[1]

[1] *Department of Condensed Matter Physics, The Weizmann Institute of Science, Rehovot 76100, Israel.*
[2] *Institut für Theoretische Festkörperphysik, Universität Karlsruhe, D–76128 Karlsruhe, Germany.*
[3] *Dahlem Center for Complex Quantum Systems and Fachbereich Physik, Freie Universität Berlin, 14195 Berlin, Germany*

(Dated: September 27, 2010)

A protocol employing weak values (WVs) to obtain ultra sensitive amplification of weak signals in the context of a solid state setup is proposed. We consider an Aharonov-Bohm interferometer where both the orbital and the spin degrees of freedom are weakly affected by the presence of an external charge to be detected. The interplay between the spin and the orbital WVs leads to a significant amplification even in the presence of finite temperatures, voltage, and external noise.

PACS numbers: 85.75.-d, 03.65.Ta 03.65.Yz, 73.63.Nm,

Weak values (WVs) were introduced more than twenty years ago [1] as a peculiarity of quantum mechanics, where the weak measurement of a component of the spin of a spin-1/2 particle can turn out to be 100, far outside the eigenvalue range of the measurement operator. A WV measurement consists in: (i) initializing the *system* in a certain state $|\psi_i\rangle$ — *pre-selection*; (ii) coupling weakly an observable $\hat{A}$ of the system with an observable $\hat{B}$ of the *detector* (via a Von Neumann interaction [2]); and (iii) retaining the detector output only if the system is eventually measured to be in a chosen final state, $|\psi_f\rangle$ — *post-selection*. The average signal detected by the detector will then be proportional to the WV

$$ {}_f\langle\hat{A}\rangle_i = \frac{\langle\psi_f|\,\hat{A}\,|\psi_i\rangle}{\langle\psi_f|\,\psi_i\rangle}\,, \tag{1}$$

rather than to the standard average value, $\langle\psi_i|\,\hat{A}\,|\psi_i\rangle$.

Going beyond the peculiarities of WV protocols, recent series of works explored the potential of WVs in quantum optics [3–6] and solid state physics [7–9], ranging from their experimental observation to the application to hyper-sensitive measurements.

Most interestingly it has been realized in the quantum optics context that a measurement, performed by a detector *entangled* with a system whose states can be pre- and post-selected, leads to an amplified signal in the detector that enables sensing of small, otherwise unaccessible quantities, e.g. sensing the deflection angle of a mirror of the order of ~ 500 femtoradians [6]. Within such a WV amplification protocol only a subset of the detector's readings — associated with the tail of the signal's distribution — is accounted for. Yet, the large value of ${}_f\langle\hat{A}\rangle_i$ outweighs the scarcity of the data points and leads to signal-to-noise ratio (SNR) amplification [10].

Here we present a paradigm WV hyper-sensitive measurement in the context of solid state systems. It consists of a open semiconducting Aharonov-Bohm (AB) interferometer subject to a Zeeman magnetic field contacted to half-metallic (strong ferromagnetic) leads. Such a device is employed to sense a small charge, q, situated next to one of the arms of the interferometer (cf. Fig. 1(a)); q affects the electron trajectory and momentum in this interferometer arm. This implies an electron spin rotation in course of the altered orbital motion of the electron (mind the magnetic field). We thus have two degrees of freedom — orbital and spin — which serve as the degrees of freedom of the "system" and "detector" respectively (or vice versa).

The value of q (its weak effect on the interferometer) is finally read in the current through the half-metal drain acting as a spin-valve (SV). We show that a properly chosen pre- and post-selection of interferometer states, while reducing the current at the drain, makes the spin coordinate of the transmitted electrons hyper-sensitive to the small charge. Our analysis underlines the interplay between a spin-related and an orbital-related WV. We show that even when the orbital WV, marking the amplification of the current signal absorbed in the interferometer's drain, is countered by the reduced current, our protocol can still be utilized to enhance signal-to-external-noise ratio. Our protocol may be extended to realistic multiterminal setups that can be employed experimentally.

Our interferometer is sufficiently open such that no higher windings around it occur. The electrons motion is ballistic, described by the Hamiltonian:

$$\hat{\mathcal{H}} = \frac{\hbar^2}{2m}(\hat{\mathbf{p}} - e\mathbf{A})^2 + \frac{g\mu_B}{2}\mathbf{B}\cdot\hat{\sigma}\,. \tag{2}$$

Here $\mathbf{A}$ represents an AB vector potential, and $\mathbf{B} = B_z\mathbf{e}_z$ is an *additional* magnetic field [11]. In generalized cylindrical coordinates $(\tilde{r}(\theta), \theta, z)$ [12, 13], the Hamiltonian reads

$$\hat{\mathcal{H}}_{\rm cyl} = \frac{\hbar^2}{2m}\hat{p}_\theta^2 + E_0 + \frac{g\mu_B}{2}B_z\hat{\sigma}_z\,, \tag{3}$$

where E_0 is the lowest transverse mode's energy. The eigenmodes' momenta along the wire, $p_\sigma \equiv p_\theta(\sigma)$, are given by

$$p_\sigma = \pm\sqrt{p_0^2 - \frac{g\mu_B m}{\hbar^2}B_z\sigma}, \tag{4}$$

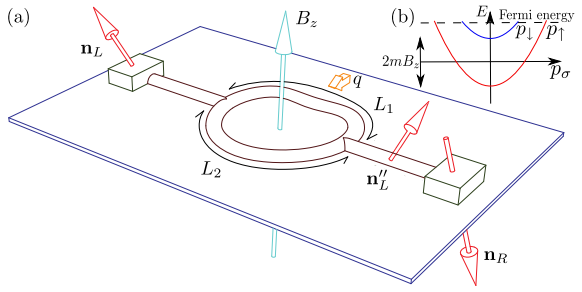

FIG. 1. (Color online) (a) A sketch of the WV hyper-sensitive charge measurement setup. It consists of a half-metal open Aharonov-Bohm interferometer with Zeeman magnetic field $\mathbf{B} = B_z\mathbf{e}_z$. The half-metal left and right leads with spin orientations $\hat{\mathbf{n}}_L, \hat{\mathbf{n}}_R$, respectively, serve as a spin-valve (SV) that measures the spin orientations of the electrons. The length of the upper (lower) arm is L_1 (L_2). The spin orientation $\hat{\mathbf{n}}''_L$ exits the right junction of the interferometer. A small charge, q, is situated next to one of the arms of the interferometer, weakly changing the confining geometry of this arm. Consequently, the electron trajectory and momentum of electrons passing through this arm are modified, inducing additional electron spin rotation which depends on whether the upper or the lower interferometer's arm is traversed (i.e., the spin is coupled to the "which-path coordinate"). The signal due to q is stored in the spin state which is read in the current through the SV. (b) A sketch of the dispersion curve for $\hat{\mathcal{H}}$, cf. Eq. (2).

where $p_0 = [(2m/\hbar^2)(E_\mathrm{F} - E_0)]^{1/2}$, and $\sigma = \pm 1 = (\uparrow, \downarrow)$ labels the spin eigenstates, $|\uparrow\rangle$, $|\downarrow\rangle$, in the direction of the applied magnetic field (cf. Fig. 1(b)).

The current, I, through the proposed ballistic device is given by the Landauer-Büttiker formula [14]

$$I = \frac{e}{h}\int dE\ |t_{L\to R}(E)|^2\,[f_L(E) - f_R(E)]\,, \qquad (5)$$

where $t_{L\to R}(E)$ is the transmission amplitude through the system at energy E, and $f_{L(R)}(E)$ is the Fermi distribution functions of the left (right) lead. Let us first discuss the effect in the case of an energy independent transmission $t_{L\to R}(E) = t_{L\to R} \equiv t_{L\to R}(E_F)$. An electron injected in a wire with spin $\sigma = \pm$, traversing a length, L, will acquire a phase $\vartheta_\sigma = p_\sigma L$. As a result, an electron injected at energy E_F, with spin $|\mathbf{n}_L\rangle$ precesses in the magnetic field, to a new spin orientation $|\mathbf{n}'_L\rangle = U(L)\,|\mathbf{n}_L\rangle = e^{i\Delta p L\hat{\sigma}_z}\,|\mathbf{n}_L\rangle$, where we have introduced $2\bar{p} \equiv p_\uparrow + p_\downarrow$, and $2\Delta p \equiv p_\uparrow - p_\downarrow$. The ferromagnetic leads form a SV, detecting the final spin orientation, with the transmission $t_{L\to R} = \langle \mathbf{n}_R|\mathbf{n}'_L\rangle$, where $|\mathbf{n}_R\rangle$ is the spin orientation of the right half-metal lead (cf. Fig. 1(a)). Passing through the interferometer's arms, L_1, L_2, an electron with spin σ has transmission amplitudes $t_{1\sigma} = |t_1|e^{i(p_\sigma L_1+\varphi_1)}$, $t_{2\sigma} = |t_2|e^{i(p_\sigma L_2+\varphi_2)}$, respectively. Hence, the transmission through our device can be written as a spin scalar product

$$T = |t_{L\to R}|^2 = \mathcal{N}^2|\langle \mathbf{n}_R|\mathbf{n}''_L\rangle|^2\,, \qquad (6)$$

where $|\mathbf{n}''_L\rangle = \langle\phi_f|U_\mathrm{int}|\phi_i\rangle\,|\mathbf{n}'_L\rangle\,/\mathcal{N}$ is a properly normalized spin state that exits the right junction with $\mathcal{N} = \sqrt{\langle \mathbf{n_L}'|\,\langle\phi_i|\,U^\dagger_\mathrm{int}\,|\phi_f\rangle\,\langle\phi_f|\,U_\mathrm{int}\,|\phi_i\rangle\,|\mathbf{n_L}'\rangle}$. Here, we have included the purely orbital effect of the interferometer (system) by defining a state that enters into the right junction of the interferometer (pre-selection), $|\phi_i\rangle = |t_1|e^{i(\bar{p}L_1+\varphi_1)}\,|1\rangle + |t_2|e^{i(\bar{p}L_2+\varphi_2)}\,|2\rangle$, and a state that comes out of it (post-selection), $|\phi_f\rangle = e^{i\Phi_\mathrm{AB}}\,|1\rangle + |2\rangle$, where $\Phi_\mathrm{AB} = -eB_z\mathcal{A}/(g\mu_\mathrm{B}\hbar)$ and $\mathcal{A}$ is the enclosed area in the AB-ring. Here $|1\rangle$ denotes an orbital wavefunction on (the l.h.s. of) arm 1. The spin rotation is the result of two contributions: first, provided the two interferometer arms are of equal length, L_2, the rotation in the applied magnetic field yields $|\mathbf{n}'_L\rangle = U(L_2)\,|\mathbf{n}_L\rangle$; second, there is an extra rotation of the component that runs through arm L_1, given by (an interplay of spin and orbit): $U_\mathrm{int} = e^{i\Delta p\Delta L\hat{A}\hat{\sigma}_z}$, with $\Delta L = L_1 - L_2$ and $\hat{A} = |1\rangle\,\langle 1|$. Henceforth, we refer to $\hat{A}$ as the which-path operator. The emerging rotated spinor is $|\mathbf{n}''_L\rangle$.

We describe, now, the effect of a *classical* charge, q, situated in the vicinity of arm 1 (for a complete description and parameters corresponding to GaAs cf. [15]). The effective electrostatic potential [16] due to the charge will modify the original confining potential, which we assume to be parabolic with curvature $m\omega_0^2$, and generated by an external gate. Assuming that the variation in the potential is adiabatic relative to the electron's longitudinal wavelength, the effect of introducing a charge results in (i) a modification of the electron's classical trajectory and (ii) an effective position-dependent parabolic potential, $V(\tilde{x}) = \Delta V(\tilde{x}) + (1/2)m(\omega_0 + \Delta\omega(\tilde{x}))^2$, where $\tilde{x}$ is the coordinate along the modified classical trajectory [15]. Since we are interested in a weak effect of the charge, at first order in q the change in the length of the modified trajectory is negligible ($\sim q^2$) while the change in the enclosed area, $\Delta\mathcal{A}$, will affect the AB-phase, $\Phi_\mathrm{AB} \to \Phi_\mathrm{AB} + \delta$. The change in energy is translated to a change in the related momenta, which, at first order in q, are $p_\sigma(\tilde{x}) = \pm\sqrt{\tilde{p}_0^2(\tilde{x}) - (g\mu_B m/\hbar^2)B_z\sigma}$, with $\tilde{p}_0(\tilde{x}) = [(2m/\hbar^2)((E_\mathrm{F}-E_0) - q(\Delta V(\tilde{x}) + (\hbar\Delta\omega(\tilde{x}))/2))]^{1/2}$. Summing it up, the effect of the charge is to modify the final spin $|\mathbf{n}''_L\rangle$ (and the corresponding normalization) in Eq. (6). It can be written in operator form

$$U_\mathrm{int} \to U^q_\mathrm{int} = e^{-iq\hat{A}\left[(\delta + \frac{m}{\bar{p}}\eta\bar{p}) - \frac{m}{\bar{p}}\eta\Delta p\hat{\sigma}_z\right]}U^{q=0}_\mathrm{int}\,, \qquad (7)$$

with $\mathcal{P} = \hbar^2 p_\uparrow p_\downarrow$, and $\eta = \int d\tilde{x}\,(\Delta V(\tilde{x}) + (\hbar\Delta\omega(\tilde{x}))/2))$. The current in the drain is sensitive to this extra spin rotation induced by the charge. The transmission through the detector in the presence of the charge is obtained by Eq. (6) with the substitutions of Eq. (7).

For simplicity, we explicitly discuss the results in the case $\Delta p\Delta L = 0 \mod (2\pi)$, in which the operator $U^{q=0}_\mathrm{int} = \mathbb{1}$ and the system and detector are coupled only due to the presence of q [17]. In a weak measurement regime the response of the detector is linear in q. Ex-

panding the exponent in Eq. (7), the change in the transmission at linear order in q is

$$\Delta T_q = T_q - T_{q=0} = -2q|\langle \mathbf{n}_R|\mathbf{n}'_L\rangle|^2|\langle\phi_f|\phi_i\rangle|^2 \times[(\delta + \frac{m}{\mathcal{P}}\eta\bar{p})\mathrm{Im}\{{}_f\langle\hat{A}\rangle_i\} - \frac{m}{\mathcal{P}}\eta\Delta p\mathrm{Im}\{{}_f\langle\hat{A}\rangle_i {}_R\langle\hat{\sigma}_z\rangle_L\}] \quad (8)$$

where we have introduced the orbital and spin WVs

$${}_f\langle\hat{A}\rangle_i = \frac{\langle\phi_f|\,\hat{A}\,|\phi_i\rangle}{\langle\phi_f|\,\phi_i\rangle} = \frac{t_1}{t_1 + t_2 e^{i\tilde{\Phi}}}\,, \quad (9)$$

$${}_R\langle\hat{\sigma}_z\rangle_L = \frac{\langle\mathbf{n}_R|\,\hat{\sigma}_z\,|\mathbf{n}'_L\rangle}{\langle\mathbf{n}_R|\,\mathbf{n}'_L\rangle} = \frac{\sum_\sigma \sigma\,\langle\mathbf{n}_R|\,\sigma\rangle\,\langle\sigma|\,\mathbf{n}'_L\rangle}{\sum_\sigma \langle\mathbf{n}_R|\,\sigma\rangle\,\langle\sigma|\,\mathbf{n}'_L\rangle}\,, \quad (10)$$

with $\tilde{\Phi} = \Phi_{\mathrm{AB}} - \bar{p}\Delta L + \varphi_2 - \varphi_1$.

In order to appreciate the enhanced sensitivity due to the post-selection in the interferometer, we focus on the simplest case ${}_f\langle\hat{A}\rangle_i \in \mathbb{R}$, where only the second term in Eq. (8) is present:

$$\Delta T_q = 2q|\langle\mathbf{n}_R|\mathbf{n}'_L\rangle|^2|\langle\phi_f|\phi_i\rangle|^2 \times \frac{m}{\mathcal{P}}\eta\Delta p_f\langle\hat{A}\rangle_i\mathrm{Im}\{{}_R\langle\hat{\sigma}_z\rangle_L\}\,. \quad (11)$$

In this case the spin emerging at the right lead of the interferometer is $|\mathbf{n}''_L\rangle \approx (\langle\phi_f|\phi_i\rangle/|\langle\phi_f|\phi_i\rangle|)\times\left(1 + iq_f\langle\hat{A}\rangle_i\frac{m}{\mathcal{P}}\eta\Delta p\hat{\sigma}_z\right)|\mathbf{n}'_L\rangle$. This spin is then projected onto $|\mathbf{n}_R\rangle$, cf. Fig. 1. Compare it with another q-detecting device made of the same SV detector but without the interferometer, where $|\mathbf{n}''_L\rangle \approx \left(1 + iq\frac{m}{\mathcal{P}}\eta\Delta p\hat{\sigma}_z\right)|\mathbf{n}'_L\rangle$. We note that in the setup with the interferometer the extra spin rotation due to the nearby charge is amplified by the WV factor ${}_f\langle\hat{A}\rangle_i$. Thus, spin rotation due to the presence of q is amplified by the WV procedure.

The story is somewhat different regarding the transmission of the orbital signal to the SV on the r.h.s.. The transmission in the simple SV case is obtained from Eq. (11) with $|t_2| = 0$, resulting in $\Delta T_q = 2q|\langle\mathbf{n}_R|\mathbf{n}'_L\rangle|^2\frac{m}{\mathcal{P}}\eta\Delta p\mathrm{Im}\{{}_R\langle\hat{\sigma}_z\rangle_L\}$. Comparing this to Eq. (8), we see that the amplification due to the which-path WV (cf. Eq. (9)) is compensated by a reduction pre-factor, $|\,\langle\phi_f|\,\phi_i\rangle\,|^2$. It turns out that tuning the interferometer to be destructive on the right junction, leading to a large ${}_f\langle\hat{A}\rangle_i$, will be countered by the reduced current.

The *relative* effect of the charge q, i.e. $(T_q - T_{q=0})/T_{q=0}$, is nevertheless enhanced by a large pre-factor ${}_f\langle\hat{A}\rangle_i$. In a similar way the sensitivity of the measurement comparing the signal with uncertainty due to an extraneous noise source is enhanced [10]. As an example we assume an uncertainty in $\mathbf{n}_R$, i.e. $|\mathbf{n}_R\rangle = \exp[i\xi\mathbf{n}_\xi\cdot\sigma]|\mathbf{n}_R\rangle$, where ξ fluctuates much slower than the time-of-flight of electrons in the device, and $\langle\xi\xi\rangle = \Delta_\xi^2$. This leads to an error in the measured change in transmission ΔT_ξ. For the simple SV case (no interferometer) $\Delta T_\xi = 2|\langle\mathbf{n}_R|\mathbf{n}'_L\rangle|^2\Delta_\xi\mathbf{n}_\xi\cdot\mathrm{Im}\{{}_R\langle\sigma_\xi\rangle_L\}$. The SNR is therefore

$$\alpha_{\mathrm{SV}} \equiv \frac{|\Delta T_q|}{|\Delta T_\xi|} = \left|\frac{qm\eta\Delta p}{\mathcal{P}\Delta_\xi}\frac{\mathrm{Im}\{{}_R\langle\hat{\sigma}_z\rangle_L\}}{\mathbf{n}_\xi\cdot\mathrm{Im}\{{}_R\langle\sigma_\xi\rangle_L\}}\right|\,. \quad (12)$$

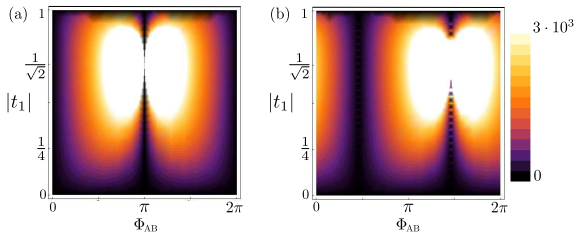

FIG. 2. (Color online) Density plot of the amplification factor, $\alpha_{\mathrm{SV+interf.}}/\alpha_{\mathrm{SV}}$, in the case of ${}_f\langle\hat{A}\rangle_i \in \mathbb{C}$ for (a) $\Delta p\Delta L = 0$ mod (2π), and (b) $\Delta p\Delta L = 2.6\cdot10^{-3}$. In both plots $\mathbf{n}_L = \mathbf{n}_R = \sigma_x$, $B_z = 1\mathrm{T}$, $\bar{p}\sim 7\cdot10^{-2}$(1/nm), $\Delta p\sim 1\cdot10^{-4}$(1/nm), $\eta\sim 207$meV·nm, $\delta\sim 1.5\cdot10^{-2}$ [15].

Considering the weak measurement device with the interferometer $\Delta T_\xi = 2\Delta_\xi|\langle\mathbf{n}_R|\mathbf{n}'_L\rangle|^2|\langle\phi_f|\phi_i\rangle|^2\mathbf{n}_\xi\cdot\mathrm{Im}\{{}_R\langle\sigma_\xi\rangle_L\}$. Assuming, again, ${}_f\langle\hat{A}\rangle_i \in \mathbb{R}$, we obtain a SNR

$$\alpha_{\mathrm{SV+interf.}} = \left|{}_f\langle\hat{A}\rangle_i\right|\alpha_{\mathrm{SV}}\,. \quad (13)$$

Since the WV, ${}_f\langle\hat{A}\rangle_i$, can be arbitrarily large, it is possible to amplify the signal at will. Indeed the post-selection due to the interferometer reduces the final current to be measured, but reduces even more the relative uncertainty on the current due to the noise-induced-error in the SV orientation (cf. Fig. 2(a)). The price to be paid for the amplification is that one has to detect smaller currents, and this sets a technical bound for the amplification.

Beyond the case ${}_f\langle\hat{A}\rangle_i \in \mathbb{R}$, the current in the detector in Eq. (8) consists of two terms. The second on the r.h.s. contains the interplay between spin and interferometer degrees of freedom leading to the WV-amplification we discussed, while the first is equivalent to the effect of the charge on a spin-less AB-interferometer times a reduction pre-factor due to the spin. The relative strength of these two terms depends on the particular values of the parameters (magnetic field, orientation of the ferromagnets, etc.), but, due to the divergence in ${}_f\langle\hat{A}\rangle_i \in \mathbb{R}$, one can always tune the interferometer's parameters to make the WV the dominant contribution. The characterization of the amplification effect in terms of the SNR, as in Eqs. (12,13), is valid in the general case (${}_f\langle\hat{A}\rangle_i \in \mathbb{C}$, $\Delta p\Delta L \neq 0 \mod (2\pi)$). We depict the amplification factor for such a general case in Fig. 2(b).

At finite temperature we cannot neglect the energy dependence of the transmission amplitude, $t_{L\to R} \to t_{L\to R}(E)$, and one needs to perform the integral over energy in Eq. (5). To do so we linearize the electron energy spectrum around the Fermi energy, in which case the energy-dependent transmission is determined by the same Eqs. (6,7) where $\bar{p} \to \bar{p}(E) = \bar{p}(1 + (m/\mathcal{P})E)$, $\Delta p \to \Delta p(E) = \Delta p(1 - (m/\mathcal{P})E)$. For details cf. [15]. As shown in Fig. 3, the low temperature and low bias voltage WV amplification in $(\alpha_{\mathrm{SV+interf.}}/\alpha_{\mathrm{SV}})$ is gradually suppressed at higher temperatures and voltage bias

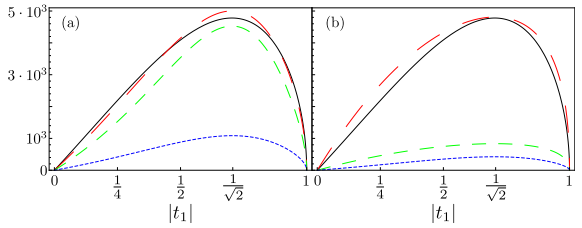

FIG. 3. (Color online) (a) The amplification factor, $\alpha_{\mathrm{SV+interf.}}/\alpha_{\mathrm{SV}}$, as a function of the transmission through arm 1 for different values of the temperature —panel (a) and voltage bias —panel (b). In panel (a) $V = 0.1$meV, and $T = 10$mK (solid,black), $T = 25$K (long dash,red), $T = 50$K (medium dash,green), $T = 100$K (short dash,blue). In panel (b) $T = 10$mK, and $V = 0.1$meV (solid,black); $V = 10$meV (long dash,red); $V = 25$meV (medium dash,green); $V = 50$meV (short dash,blue). In all plots $\Phi_{\mathrm{AB}} = \pi$ and all other parameters are chosen as in Fig. 2.

$(k_BT \sim eV \gtrsim (\mathcal{P}/m)\max\{(1/\Delta pL),(1/\bar{p}\Delta L)\})$. At $k_BT \lesssim (\mathcal{P}/m)\max\{(1/\Delta pL),(1/\bar{p}\Delta L)\}$ the signal-to-noise ratio can even be enhanced since temperature affects differently the signal and the noise.

In much the same way, Gaussian magnetic field fluctuations of width ΔB will smear the WV-amplification. We include the dependence of the transmission amplitude, $t_{L\to R} \to t_{L\to R}(B)$, and integrate over the magnetic field distribution. In a way compatible with our earlier approximation we linearize the electron energy spectrum around the tuned magnetic field, B_0, in which case the magnetic field-dependent transmission is determined by the same Eqs. (6,7) where $\bar{p} \to \bar{p}(B) = \bar{p} - \Delta p(g\mu_B m/2\mathcal{P})B$, $\Delta p \to \Delta p(B) = \Delta p + \bar{p}(g\mu_B m/2\mathcal{P})B$ (cf. Eq. (4)) [15]. As shown in Fig. 4, the amplification due to the WV is completely suppressed in the high magnetic noise limit $\Delta B\Phi_{\mathrm{AB}} \gg B$. Unlike the temperature/voltage case, here the WV amplification is suppressed predominantly by the effect of fluctuations on the AB phase, rather than dephasing due to the momenta, Δp, $\bar{p}$.

Here we have proposed a setup which exploits the notion of ultra high amplification within a weak value protocol, in the context of a quantum solid state device. An important feature of our design is that by assigning to spin and orbital degrees of freedom the meaning of a "system" and a "detector", it allows us to observe WV without synchronizing (in time) pulses in the system and the detector. Such a necessity arose in earlier proposals [7–9]. We stress that the main focus of the present work was to demonstrate conceptually that WV amplification is possible employing solid state devices. While attempt has been made to conform to realistic values of parameters [15], the present analysis does not purport to substitute a careful numerical/material science oriented analysis of an operating device.

This work was supported by GIF, DFG Center for Functional Nanostructures, Einstein Minerva Center, US-Israel BSF, ISF, Minerva Foundation, DFG SPP 1285, EU GEOMDISS, Ministry of Immigrant Absorption (Israel), Alexander von Humboldt Foundation. We would like to thank B. Nissan-Cohen and D. Klarman for fruitful discussions. We would like to thanks R. Eliav for the illustration of the device.

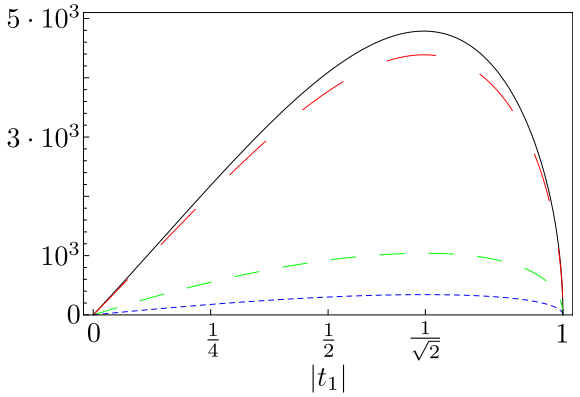

FIG. 4. (Color online) The amplification factor, $\alpha_{\mathrm{SV+interf.}}/\alpha_{\mathrm{SV}}$, as a function of the transmission through arm 1 for different strength of the magnetic field fluctuations: $\Delta B = 10$mT (solid,black), $\Delta B = 100$mT (long dash,red); $\Delta B = 500$mT (medium dash,green); and $\Delta B = 700$mT (short dash,blue). All plots are for $\Phi_{\mathrm{AB}} = \pi$ and all the other parameters are chosen as in Fig. 2.

[1] Y. Aharonov, D. Z. Albert, and L. Vaidman, Phys. Rev. Lett. **60**, 1351 (1988).
[2] J. von Neumann, *Mathematical Foundation of Quantum Theory* (Princeton, University Press, New Jersey, 1938).
[3] N. W. M. Ritchie, J. G. Story, and R. G. Hulet, Phys. Rev. Lett. **66**, 1107 (1991).
[4] G. J. Pryde, J. L. O'Brien, A. G. White, T. C. Ralph, and H. M. Wiseman, Phys. Rev. Lett. **94**, 220405 (2005).
[5] O. Hosten and P. Kwiat, Science **319**, 787 (2008).
[6] P. B. Dixon, D. J. Starling, A. N. Jordan, and J. C. Howell, Phys. Rev. Lett. **102**, 173601 (2009).
[7] N. S. Williams and A. N. Jordan, Phys. Rev. Lett. **100**, 026804 (2008).
[8] A. Romito, Y. Gefen, and Y. M. Blanter, Phys. Rev. Lett. **100**, 056801 (2008).
[9] V. Shpitalnik, Y. Gefen, and A. Romito, Phys. Rev. Lett. **101**, 226802 (2008).
[10] D. J. Starling, P. B. Dixon, A. N. Jordan, and J. C. Howell, Phys. Rev. A **80**, 041803 (2009).
[11] Generalizations into setups which include both a magnetic field and spin–orbit coupling can be made along the lines of Ref. [13], as q only affects the accumulated dynamic phase along the interferometer arms.
[12] F. E. Meijer, A. F. Morpurgo, and T. M. Klapwijk, Phys. Rev. B **66**, 033107 (2002).
[13] R. S. Whitney, A. Shnirman, and Y. Gefen, Phys. Rev. Lett. **100**, 126806 (2008).

[14] M. Blanter and M. Büttiker, Phys. Rep. **336**, 1 (2000).
[15] See Supplementary Material.
[16] T. Ando, A. B. Fowler, and F. Stern, Rev. Mod. Phys. **54**, 437 (1982).
[17] In the general case we will obtain similar amplification as in this simplified case (cf. Fig. 2(b)).

Supplementary Material I: Electrostatic effect of a charge placed next to an electron wire

We describe, here, the effect of a classical charge in the vicinity of arm 1 of the AB-ring. We use an electrostatic model and plug realistic numbers for a GaAs system. The arm is treated as a straight wire in the vicinity of the charge (see Fig. 5, described by a parabolic confining potential at a distance, l, from the $\hat{x}$-axis, $V_{\rm har}(x,y) = (1/2)m\omega_0^2(y-l)^2$. We include only the lowest transverse mode by tuning ω_0 such that $E_f \approx \hbar\omega_0$. The charge is situated at the origin and is modeled with a two-dimensional electron gas electrostatic potential, $V_e(x,y) = (qe^2)/(\bar{k}\bar{q}_s^2 r^3)$, where $\bar{k}$ is the dielectric constant, $\bar{q}_s$ a screening parameter, and $r = \sqrt{x^2+y^2}$ [16]. Taking $V = V_{\rm har} + V_e$ and its derivatives $\vec{V} = (V_x, V_y), V_{xx}, V_{xy}, V_{yx}, V_{yy}$, we find the new electron trajectory by defining two constraints for each point along the trajectory: (i) the point is the local minimum in a given ϕ direction, i.e. $\vec{\nabla}\cdot\vec{V}^{\phi} = V_y - \tan(\phi)V_x = 0$; (ii) the curvature is quadratic in the given direction, i.e. the off-diagonal terms in the rotated Hessian are zero $(V_{yy} - V_{xx})\tan(2\phi) + 2V_{xy} = 0$. Combining the two conditions we obtain the function

$$F(x,y,q) = V_y - \left(\frac{\sqrt{1+T^2}-1}{T}\right)V_x \equiv 0\,, \qquad (14)$$

where we have used the trigonometric relation $\tan(2\phi) = 2\tan(\phi)/(1-\tan(\phi)^2)$ to define $T = \tan(2\phi) = V_{xy}/(V_{xx}-V_{yy})$. Solving Eq. 14 perturbatively in q, i.e. $y \approx l + qy_1(x)$, we obtain the added trajectory due to the charge

$$y_1(x) = -\frac{F_q|_{q=0}}{F_y|_{q=0}}\,, \qquad (15)$$

where we have defined the function's derivatives F_q, F_y. An electron traveling in this new trajectory will feel a position dependent minimum potential, $\Delta V(x) = V(x, l+qy_1(x))$, and a changed local confining potential in the transverse direction $m\omega_0'(x) = m\omega_0 + q\Delta\omega(x) = V_{yy}^{\phi} = \left((1/(1+T^2))(V_{yy} + T^2V_{xx} - 2TV_{xy})\right)|_{y=l+qy_1(x)}$. Plugging these changes into Eq. 4 we obtain a local linear correction to the eigenmomenta $p_\sigma(x) = \pm\sqrt{\tilde{p}_0^2(x) - \frac{g\mu_B}{2}mB_z\sigma}$, with $\tilde{p}_0(x) = [2m((E_{\rm F}-E_0) - q(\Delta V(x) + (\hbar\Delta\omega(x))/2))]^{1/2}$. The overall effect is obtained by integrating over the difference in accumulated dynamical phase over new trajectory

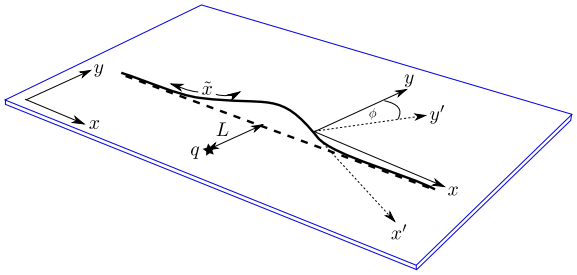

FIG. 5. (Color online) The effect of a classical charge, q, on the electron's trajectory.

$$\int_\gamma p_\sigma(\gamma)\cdot d\vec{l} = \int_{-\infty}^{\infty} dx(p_\sigma(x)\sqrt{1+q^2(y_1'(x))^2} - p_\sigma)$$
$$\approx -\frac{qmp_{\bar{\sigma}}}{\mathcal{P}}\int_{-\infty}^{\infty} dx\Delta V(x) + (\hbar\Delta\omega(x))/2) \equiv -\frac{qmp_{\bar{\sigma}}}{\mathcal{P}}\eta\,, \qquad (16)$$

where we use the fact the change in the length of the modified trajectory is negligible ($\sim q^2$). Additionally, the new trajectory encloses a different area, $\Delta\mathcal{A} = \int_{-\infty}^{\infty} dx\; y_1(x)$, which will affect the accumulated AB-phase $\Phi_{\rm AB} \to \Phi_{\rm AB} + \delta$.

In GaAs $E_f \cong 10$meV, therefore, we choose $\omega_0 \sim 15$THz, which is equivalent to a wire width of ~ 19.5nm. The dielectric constant is $\bar{k} = 12.9$ and the screening length $l_s = 1/q_s \sim 8.5$nm. We take the charge's distance from the wire to be $l = 3l_s \sim 25.5$nm with a wire length $L = 1\mu$m. For a magnetic field of $B_z \sim 1$T, this results in $\bar{p} \sim 7\cdot 10^{-2}(1/\text{nm})$, $\Delta p \sim 1\cdot 10^{-4}(1/\text{nm})$, $\eta \sim 207$meV·nm, $\delta \sim 1.5\cdot 10^{-2}$.

Supplementary Material II: Finite energy and magnetic fluctuations

The WV signal is sensitive to temperature, voltage bias, and magnetic field fluctuations. However, it still survives to generate an amplification in reasonable ranges of parameters. We consider the effect of each of these factors separately. The energy and temperature dependence of the transmission is calculated by plugging, $t_{L\to R} \to t_{L\to R}(E)$, into Eq. (5) and performing the integrals. Similarly, with $t_{L\to R} \to t_{L\to R}(B)$, we integrate over a Gaussian distribution of width ΔB around the original magnetic field B_0. To solve the energy (magnetic field) integral, we linearize the momenta around E_f (B_0), i.e. $\bar{p} \to \bar{p}(E) = \bar{p}(1 + (m/\mathcal{P})E)$, $\Delta p \to \Delta p(E) = \Delta p(1 - (m/\mathcal{P})E)$ ($\bar{p} \to \bar{p}(B) = \bar{p} - \Delta p(g\mu_B m/2\mathcal{P})B$, $\Delta p \to \Delta p(B) = \Delta p + \bar{p}(g\mu_B m/2\mathcal{P})B$). Additionally, $\Phi_{\rm AB}, \delta \to \Phi_{\rm AB}(B), \delta(B)$ depends on the magnetic field fluctuations. In Eq. (8) the dependence of ΔT_q on energy and magnetic field is due to the following terms: $|\langle \mathbf{n}_R|\mathbf{n}_L'\rangle|^2 = \sum_\sigma |\langle\sigma|\mathbf{n}_R\rangle|^2|\langle\sigma|\mathbf{n}_L\rangle|^2 +$

$2\mathrm{Re}\left\{e^{i2\Delta p(E,B)L}\langle\mathbf{n}_L|\downarrow\rangle\langle\downarrow|\mathbf{n}_R\rangle\langle\mathbf{n}_R\uparrow\rangle\langle\uparrow|\mathbf{n}_L\rangle\right\}$, $|\langle\phi_f|\phi_i\rangle|^2{}_f\langle\hat{A}\rangle_i = t_1^2 + t_1t_2e^{-i\tilde{\Phi}(E,B)}$, and $|\langle\mathbf{n}_R|\mathbf{n}'_L\rangle|^2{}_R\langle\hat{\sigma}_z\rangle_L = \sum_\sigma \sigma|\langle\sigma|\mathbf{n}_R\rangle|^2|\langle\sigma|\mathbf{n}_L\rangle|^2 + 2i\mathrm{Im}\left\{e^{i2\Delta p(E,B)L}\langle\mathbf{n}_L|\downarrow\rangle\langle\downarrow|\mathbf{n}_R\rangle\langle\mathbf{n}_R\uparrow\rangle\langle\uparrow|\mathbf{n}_L\rangle\right\}$. Performing the integral over the E and B windows, we obtain

$$\Delta T_q(T,V) = -2qeV(\delta+\frac{m}{\mathcal{P}}\eta\bar{p})t_1t_2(\sum_\sigma|\langle\sigma|\mathbf{n}_R\rangle|^2|\langle\sigma|\mathbf{n}_L\rangle|^2\mathrm{Im}\{e^{-i\tilde{\Phi}}K(T,V,\bar{p}\Delta L)\}$$
$$+|\langle\mathbf{n}_L|\downarrow\rangle\langle\downarrow|\mathbf{n}_R\rangle\langle\mathbf{n}_R\uparrow\rangle\langle\uparrow|\mathbf{n}_L\rangle|(\mathrm{Im}\{e^{i(2\Delta pL-\varphi-\tilde{\Phi})}K(T,V,-(\Delta pL+\bar{p}\Delta L))\}-\mathrm{Im}\{e^{i(2\Delta pL-\varphi+\tilde{\Phi})}K(T,V,(\bar{p}\Delta L-\Delta pL))\}))$$
$$+2qeV\frac{m}{\mathcal{P}}\eta\Delta p(2t_1^2|\langle\mathbf{n}_L|\downarrow\rangle\langle\downarrow|\mathbf{n}_R\rangle\langle\mathbf{n}_R\uparrow\rangle\langle\uparrow|\mathbf{n}_L\rangle|\mathrm{Im}\{e^{i(2\Delta pL-\varphi)}K(T,V,-\Delta pL)\}$$
$$+t_1t_2(\sum_\sigma\sigma|\langle\sigma|\mathbf{n}_R\rangle|^2|\langle\sigma|\mathbf{n}_L\rangle|^2\mathrm{Im}\{e^{-i\tilde{\Phi}}K(T,V,\bar{p}\Delta L)\}$$
$$+|\langle\mathbf{n}_L|\downarrow\rangle\langle\downarrow|\mathbf{n}_R\rangle\langle\mathbf{n}_R\uparrow\rangle\langle\uparrow|\mathbf{n}_L\rangle|(\mathrm{Im}\{e^{i(2\Delta pL-\varphi-\tilde{\Phi})}K(T,V,-(\Delta pL+\bar{p}\Delta L))\}+\mathrm{Im}\{e^{i(2\Delta pL-\varphi+\tilde{\Phi})}K(T,V,(\bar{p}\Delta L-\Delta pL))\}))),$$
$$\Delta T_q(\Delta B) = -2qeV(\delta+\frac{m}{\mathcal{P}}\eta\bar{p})t_1t_2(\sum_\sigma|\langle\sigma|\mathbf{n}_R\rangle|^2|\langle\sigma|\mathbf{n}_L\rangle|^2\mathrm{Im}\{e^{-i\tilde{\Phi}}F(\Delta B,e\mathcal{A}/(g\mu_\mathrm{B}\hbar)-\frac{m}{2\mathcal{P}}\Delta p\Delta L)\}$$
$$+|\langle\mathbf{n}_L|\downarrow\rangle\langle\downarrow|\mathbf{n}_R\rangle\langle\mathbf{n}_R\uparrow\rangle\langle\uparrow|\mathbf{n}_L\rangle|\times$$
$$(\mathrm{Im}\{e^{i(2\Delta pL-\varphi-\tilde{\Phi})}F(\Delta B,e\mathcal{A}/(g\mu_\mathrm{B}\hbar)+\frac{m}{2\mathcal{P}}(2\bar{p}L-\Delta p\Delta L))\}$$
$$-\mathrm{Im}\{e^{i(2\Delta pL-\varphi+\tilde{\Phi})}F(\Delta B,-e\mathcal{A}/(g\mu_\mathrm{B}\hbar)+\frac{m}{2\mathcal{P}}(2\bar{p}L+\Delta p\Delta L))\}))$$
$$+2qeV\frac{m}{\mathcal{P}}\eta\Delta p(2t_1^2|\langle\mathbf{n}_L|\downarrow\rangle\langle\downarrow|\mathbf{n}_R\rangle\langle\mathbf{n}_R\uparrow\rangle\langle\uparrow|\mathbf{n}_L\rangle|\mathrm{Im}\{e^{i(2\Delta pL-\varphi)}F(\Delta B,\frac{m}{2\mathcal{P}}\bar{p}L)\}$$
$$+t_1t_2(\sum_\sigma\sigma|\langle\sigma|\mathbf{n}_R\rangle|^2|\langle\sigma|\mathbf{n}_L\rangle|^2\mathrm{Im}\{e^{-i\tilde{\Phi}}F(\Delta B,e\mathcal{A}/(g\mu_\mathrm{B}\hbar)-\frac{m}{2\mathcal{P}}\Delta p\Delta L)\}$$
$$+|\langle\mathbf{n}_L|\downarrow\rangle\langle\downarrow|\mathbf{n}_R\rangle\langle\mathbf{n}_R\uparrow\rangle\langle\uparrow|\mathbf{n}_L\rangle|\times$$
$$(\mathrm{Im}\{e^{i(2\Delta pL-\varphi-\tilde{\Phi})}F(\Delta B,e\mathcal{A}/(g\mu_\mathrm{B}\hbar)+\frac{m}{2\mathcal{P}}(2\bar{p}L-\Delta p\Delta L))\}$$
$$+\mathrm{Im}\{e^{i(2\Delta pL-\varphi+\tilde{\Phi})}F(\Delta B,-e\mathcal{A}/(g\mu_\mathrm{B}\hbar)+\frac{m}{2\mathcal{P}}(2\bar{p}L+\Delta p\Delta L))\})),$$

where we have used the azimuth phase difference between the pre- and post-selected spin orientations φ, the function $K(T,V,N) = \frac{2\pi}{\beta eV}e^{i\frac{eVmN}{2\mathcal{P}}}\frac{\sin\left(\frac{eVmN}{2\mathcal{P}}\right)}{\sinh\left(\frac{\pi mN}{\mathcal{P}\beta}\right)}$, and $F(\Delta B,N) = e^{-\frac{1}{2}(\Delta BN)^2}$. It results in smearing of the signal (cf. Fig. 3,4).